



Electrochemical sensor based on CuO/reduced graphene nanoribbons and ionic liquid for simultaneous determination of tramadol, olanzapine and acetaminophen

Hamed Shahinfard¹ · Mehdi Shabani-Nooshabadi^{1,2} · Adel Reisi-Vanani¹ · Rozhin Darabi²

Received: 9 December 2022 / Revised: 1 March 2023 / Accepted: 4 April 2023 / Published online: 19 April 2023
© The Author(s), under exclusive licence to Korean Carbon Society 2023

Abstract

In the present investigation, a new electrochemical sensor based on carbon paste electrode was applied to simultaneous determine the tramadol, olanzapine and acetaminophen for the first time. The CuO/reduced graphene nanoribbons (rGNR) nanocomposites and 1-ethyl 3-methyl imidazolium chloride as ionic liquid (IL) were employed as modifiers. The electro-oxidation of these drugs at the surface of the modified electrode was evaluated using cyclic voltammetry (CV), differential pulse voltammetry (DPV), electrochemical impedance spectroscopy (EIS) and chronoamperometry. Various techniques such as scanning electron microscopy (SEM) with energy dispersive X-Ray analysis (EDX), X-ray diffraction (XRD) and fourier-transform infrared spectroscopy (FTIR), were used to validate the structure of CuO-rGNR nanocomposites. This sensor displayed a superb electro catalytic oxidation activity and good sensitivity. Under optimized conditions, the results showed the linear in the concentration range of 0.08–900 μM and detection limit (LOD) was achieved to be 0.05 μM . The suggested technique was effectively used to the determination of tramadol in pharmaceuticals and human serum samples. For the first time, the present study demonstrated the synthesis and utilization of the porous nanocomposites to make a unique and sensitive electrode and ionic liquid for electrode modification to co-measurement of these drugs.

Keywords Electrochemical sensor · Carbon paste electrode · Tramadol · Ionic liquid · Graphene nanoribbons

1 Introduction

Tramadol, (1R, 2R)-2-[(dimethylamino) methyl]-1-(3-methoxyphenyl) cyclohexanol as an analgesic extensively employed for the treatment of moderate to severe pain. Tramadol blocks the transmission of pain signal to brain by blocking the opioid receptors and also as an inhibitor reuptake of norepinephrine and serotonin neurotransmitter. However, the excessive consumption of Tramadol influences the central nervous system and lead to risk of mortality and unpleasant consequences, such as slowness or ceased breath and heart problems and even death [1, 2]. Olanzapine 2-methyl-4-(4-methyl-1-piperazynyl)10H-thieno- [2,3 b] [1, 5] benzodiazepine is used

to the stress treatment and remedy schizophrenia and bipolar disease. Long-term consumption of this drug may cause in syndrome serotonin. Olanzapine molecule is considered a new unusual neuroleptic because it has a great dependency for D_2 dopamine and $5H_2$ serotonin as two receptors in the brain for continuing chemical balance in the brain [3–6]. Acetaminophen (4'-hydroxyacetanilide, *N*-acetyl *p*-aminophenol, paracetamol) as a pain reliever is extensively applied to fever, headache and over the counter analgesic. The excessive consumption of Acetaminophen may lead to severe diseases because of produce the accumulation of toxic [7–11]. The simultaneous consumption of Tramadol and Acetaminophen could be improved the influence of Tramadol in relieve pain, whereas the excessive consumption may include side effects which lead to toxicity. Antagonistic activity of olanzapine in comparison with other antipsychotic drugs is more on serotonin, dopaminergic and adrenergic receptors [4]. While Tramadol obtained low risk of addiction but it can consider as inhibitor serotonin reuptake and could be increased dose of serotonin which leading to syndrome of serotonin. As a result

✉ Mehdi Shabani-Nooshabadi
m.shabani@kashanu.ac.ir

¹ Institute of Nano Science and Nano Technology, University of Kashan, Kashan, Iran

² Department of Analytical Chemistry, Faculty of Chemistry, University of Kashan, Kashan, Iran

the simultaneous measurement of Olanzapine, Acetaminophen and Tramadol in clinical samples is important [12].

Up to now several analytical techniques such as HPLC [2, 13, 14], LC–MS/MS [15–17], SERs [18–20], GC–MS [21], colorimetric [22, 23] and electrochemical techniques [24–28] was employed to determine Olanzapine, Acetaminophen and Tramadol. Among techniques, electrochemical methods have more attractive due to beneficial features such as fast response, high sensitivity and low cost [29–37]. Modification of CPE with nanomaterial could be overcome on undesired features such as slow electron transfer rate, slow response and low sensitivity [38–40]. Cupric oxide (CuO) was used in the present work mainly because of its eco-friendly nature, low-cost and its frequent been widely applied in many fields. The important p-type metal oxide as an important p-type metal oxide semiconductor has a narrow band gap (Eg $\frac{1}{4}$ 1.2 eV/1.5 eV). Recently, metal oxide/graphene hybrids, have attracted increasing attention because of their improved electrochemical performance [41, 42]. Among different carbon-based nanomaterial graphene nanoribbon (GNR) as a new type of conductive materials have reached more attention in sensing platforms, in compared with other carbon-based nanostructures. GNR have opened new avenue toward extended potential to react with so many nanoparticles in various fields. The features of GNR are dependent on edge structure and type of functional groups including the carbonyl (–CO), carboxyl (–COOH), hydrogenated (–CH), and amines (–NH₂) that have attached on GNR's edges [43]. In electrochemical investigation, GNR is a suitable choice because of some unique attributes such as large specific surface area, fast electron rate because of many edge and defects existed in GNR structure and extended potential window in determination of various analytes [44, 45]. Room temperature ionic liquids (RTILs) as known ionic solvent are combination of equal electropositive asymmetrical organic cations and electronegative organic/inorganic anions with molten point less than room temperature. Among ILs, 1-ethyl 3-methyl imidazolium chloride is widely applied for electrochemical purposes because of outstanding properties such as negligible vapor pressure, thermal stability and recyclability [46]. In this investigation, a new modified sensor based on CuO-rGNR and ionic liquid (IL) exhibited excellent sensitivity toward measurement of Tramadol in biological samples. Proposed nanostructure with some attributes such as high surface-area, great conductivity and superior electro-catalytic behavior could be used as suitable modifier for working electrode in electrochemical measurements of these drugs for the first time.

2 Experiments

2.1 Chemicals and reagent

All chemicals utilized in this study were of analytical grade. Ethanol, paraffin oil, graphite powder, copper acetate (Cu (CH₃COO)₂), acetic acid (CH₃COOH), sodium hydroxide (NaOH), carbon nano tube (CNT), sulfuric acid (H₂SO₄), potassium permanganate (KMnO₄), phosphoric acid (H₃PO₄), hydrogen peroxide (H₂O₂) and other chemicals used were got from Merck. A stock solution with a concentration of 0.1 M was applied to prepare several concentrations of Tramadol. Phosphate buffer solutions (PBS) were employed as supporting electrolytes with a concentration 0.1 M were ready from sodium hydroxide and H₃PO₄ to adjusted the pH value (pH from 3.0 to 9.0). Employed drugs were supplied from Merck with high purity. 1-ethyl 3-methyl imidazolium chloride was acquired from Sigma–Aldrich with 99% Purity. Phosphoric acid (85% Purity) and sodium hydroxide (0.1 M) (85% Purity) was employed to adjust pH value of the prepared phosphate buffer solution (PBS). The pure graphite powder (%99 purity) and high viscosity paraffin oil (> 99%) were obtained from Merck.

2.2 Apparatus and instruments

Electrochemical signals were achieved by the Autolab PGSTAT 302 N electrochemical device consist of three electrodes. In this system modified carbon paste electrode as working electrode, a saturated Ag / AgCl / KCl_{sat} and platinum-wire were employed as reference and auxiliary electrodes, respectively; various pH values were attained by Metrohm pH meter made in Switzerland. Scanning electron microscopy (Mira3Tescan SEM) and X-ray powder diffraction (STOE diffractometer with Cu – K_a radiation) were employed to characterize the synthesized CuO-rGNR.

2.3 Synthesis of CuO/rGNR nanocomposite

The CuO nanoparticles were synthesized using a facile method [47]. In brief, a mix of acetic acid (2 ml) and copper acetate (0.2 M) was heated up to the boiling point. After that 30 ml of sodium hydroxide (8 M) was added the mixture. Then the solution was stirred at the boiling point for 2 h. After cooling down to room temperature, the black precipitate obtained (CuO-nanoparticles) was washed with distilled water several times. The unzipping method was used for the synthesis of GNR. In brief 100 mg of functionalized MWCNT was added to a beaker containing 180 ml of sulfuric acid (H₂SO₄). The suspension was

stirred for 1 h. Phosphoric acid (85%, 20 mL) was added to mixture and the solution was stirred for 20 min. After that 6 g of potassium permanganate (KMnO_4) was added into the solution slowly. The resulting mixture was heated up to 328 K and stirred for another 2 h. After cooling down to room temperature, 100 ml of DI water which contained 2 ml of hydrogen peroxide (H_2O_2) was poured into the solution. The result mixture was centrifuged and washed with HCl and acetone several times, and the precipitate obtained was dried at 333 K [48, 49]. For the synthesis of CuO-rGNR nanocomposite a mix of synthesized CuO and synthesized GNR with mass ratios of 1: 2 was transferred into a beaker consist of 20 ml of ethanol and stirred for 1 h. then the heterogeneous mixture obtained transferred into a Teflon-lined stainless-steel autoclave and heated at 453 K temperature for 18 h. The mixture was washed with a mixture of DI water and ethanol several time and dried at 333 K.

2.4 Fabrication of modified electrode

To achieve the modified electrode, the IL/CuO-rGNR/CPE (0.10 g) was added to mixing of 0.99 g of graphite powder with paraffin oil at a ratio of 70:30 (w/w). After that 0.1 ml 1-ethyl-3-methylimidazolium chloride were added to the attained carbon paste. The IL/CuO-rGNR/CPE was packed into a glass tube with a copper wire to obtained electrical contact and it was employed as a working electrode.

2.5 Real samples fabrication

To preparation of real sample, the amount of 1 ml of fresh human plasma or human urine samples was diluted 10 times by 0.1 M of PBS (pH 7.0). To dissolve the real sample of the tablet, a certain amount of tramadol tablet was dissolved in deionized water (DI water) and it was diluted in 10 ml of PBS at pH = 7.0. For diluted samples, a 0.45- μm membrane filter was applied.

3 Result and discussion

3.1 Characterization of CuO-rGNR

The morphological investigation of CuO-rGNR was distinguished by SEM micrographs at various scales. As shown in Fig. 1A–C, the images indicated that the CuO nanoparticle distributed on GNR layers. It was showed that GNR act as a supportive sheet for CuO nanoparticles. The existence of Cu, O and C elements in CuO-rGNR nanocomposite was revealed by EDX analysis (Fig. 1D). As can be seen in the XRD pattern of CuO-rGNR as shown in Fig. 1E, there was no any characteristic peak related to GNR, it can be

attributed to reduction process of GNR to r-GNR which remove the oxygen functional groups of GNR. The sharp peaks were observed at $34^\circ, 36^\circ, 39^\circ, 49^\circ, 58^\circ, 62^\circ, 68^\circ, 74^\circ$ and 76° corresponding crystal planes for CuO. The peak at about 15° was corresponded to CuO-GNR interaction process.

Based on the obtained FTIR spectrum (Fig. 1F) the absorption peak at 1104 cm^{-1} and 1451 cm^{-1} , was related to C–O, C–OH, respectively, and the peak appeared at 1644 cm^{-1} can be corresponded to C=O, both intermolecular and intramolecular hydrogen bonding with hydroxyl groups cause to downshift in the C=O stretching mode. Also the board band from 3431 cm^{-1} could be assigned to stretch of O–H. The result of FTIR included many functional groups. Also, the peak obtained at 484 cm^{-1} was recognized to the stretching band of Cu–O from CuO-rGNR nanocomposite [49, 50].

3.2 Electrochemical investigations

The electro oxidation of 500 μM of Tramadol was studied through CV technique on the surface of proposed sensor (IL/CuO-rGNR/CPE) at different pH range (from 3 to 9). Figure 2A, illustrated as pH values were changed from 3 to 7, and the I_p of Tramadol was increased. I_p was decreased at the pH values higher than 7. So, pH = 7 was elected as optimum pH. Also, with increasing pH values, the oxidation peak of potential (E_p) was shifted to negative values. It can be concluded the H^+ ions can be contributed in the oxidation of tramadol at the surface of IL/CuO-rGNR/CPE and electrochemical behavior of Tramadol depends on the amount of proton in the solution. As demonstrated in Fig. 2B, there was a linear correlation for plot of E_p vs pH with slope value of -0.034 E/pH ($R^2 = 0.9983$), and regarded to the Nernst equation ($E = E^0 - \frac{\alpha RT}{nF} p\text{H}$), to calculate the mechanism of electron transfer in the electro-oxidation process of Tramadol, the number of electrons was twice than the proton which are contributed in the electrochemical process ($n = 2$). CV technique was employed to investigate of the electro oxidation behavior of Tramadol at the surface of CPE and various modified electrodes including (CPE, CuO/CPE, GNR/CPE, CuO-GNR/CPE, IL/CPE, IL/CuO-rGNR/CPE) in PBS at pH = 7. As shown in Fig. 3, no reduction peak was existed in the reverse scan, which showed the oxidation of Tramadol on the surface of electrodes was irreversible. Besides, the largest peak current (I_p) with value of $41.67\text{ }\mu\text{A}$ was obtained for IL/CuO-rGNR/CPE comparison with the I_p of CPE with value of $17.2\text{ }\mu\text{A}$. The current density of CPE (a), CuO/CPE(b), GNR/CPE(c), CuO-GNR/CPE (d), IL/CPE(e), IL/CuO-rGNR/CPE (f) in the presence of 500 μM Tramadol at pH 7.0 and scan rate of 50 mV s^{-1} , were obtained 237.29, 345.71, 484.29, 488, 525.29 and 591.43, respectively. It can be concluded modifying CPE with nanocomposite and ionic liquid improved the active surface area

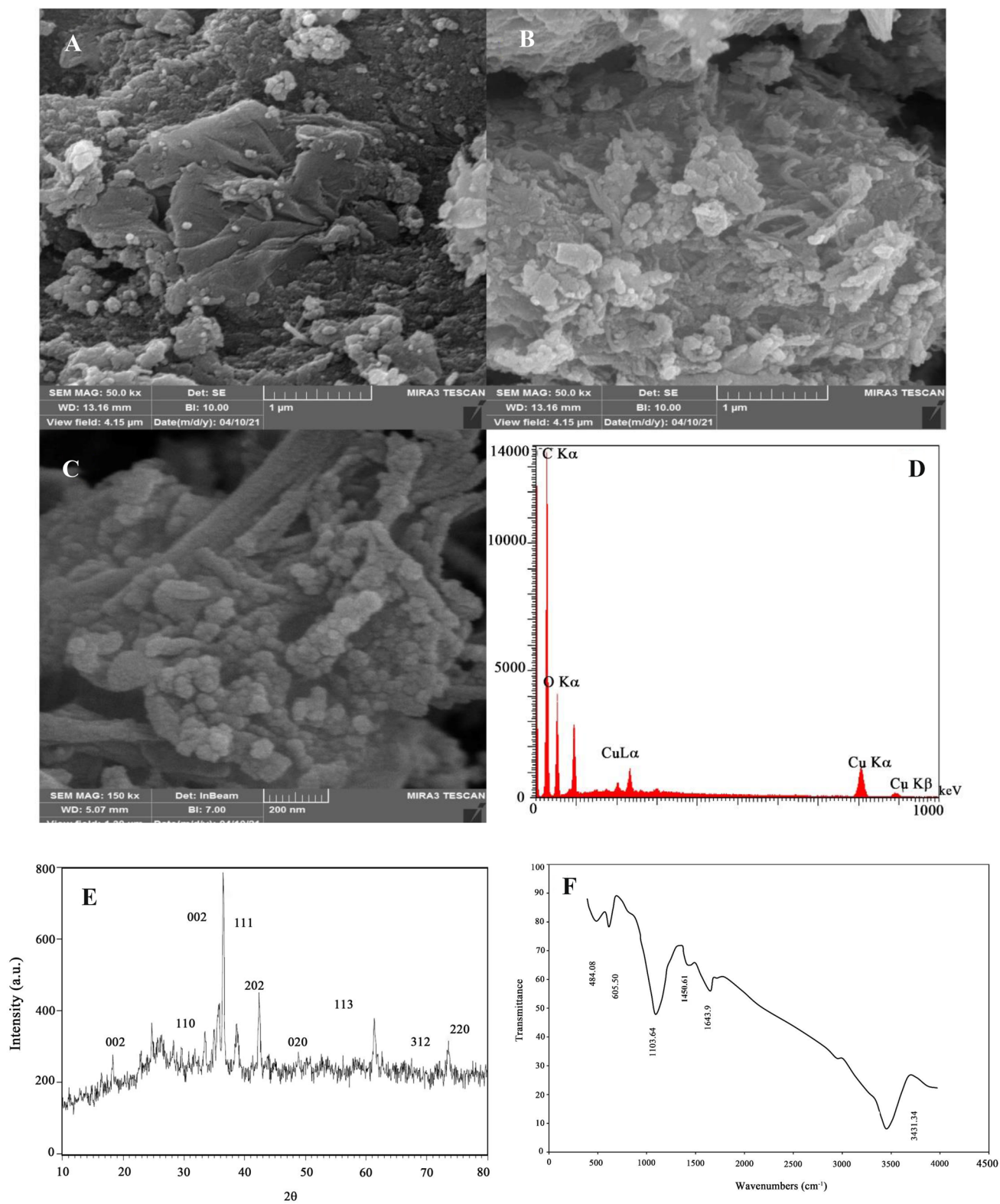


Fig. 1 The SEM micrographs (A–C), EDX (D), XRD patterns (E) and FT-IR analysis (F) of as-synthesized IL/CuO-rGNR/CPE

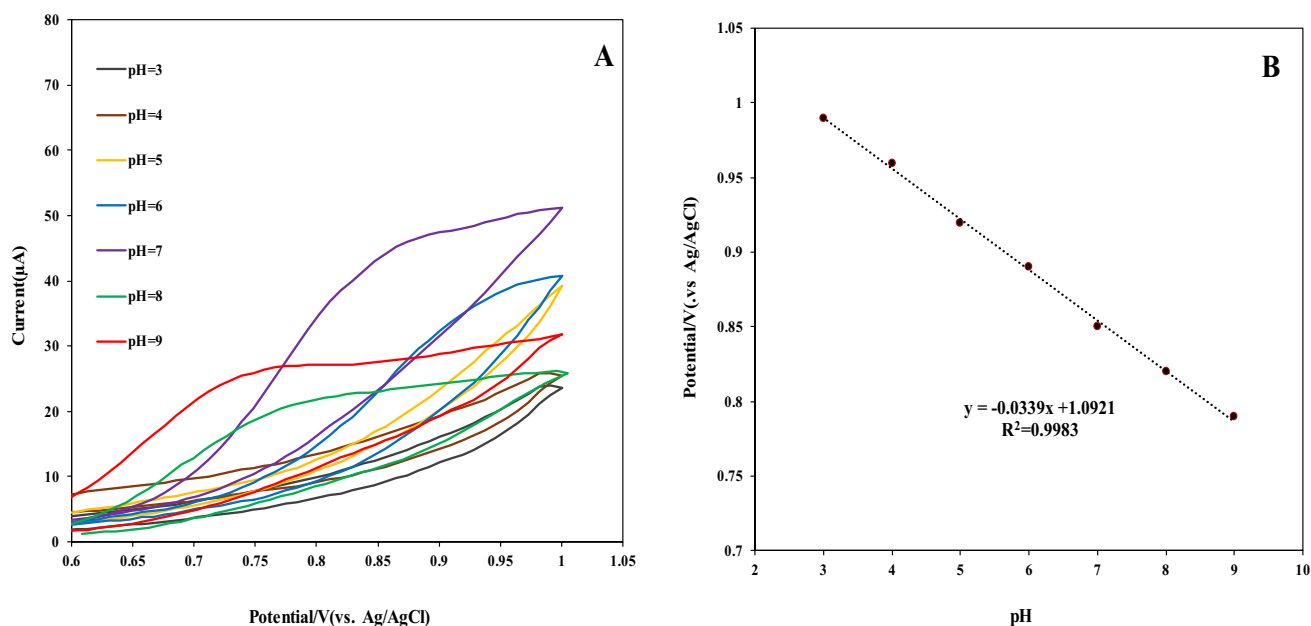


Fig. 2 The effect of pH on CV of Tramadol at a surface of the IL/CuO-rGNR/CPE (pH 3–9, respectively) (A) and E. vs. pH for the electro-oxidation of 500 μM Tramadol at a surface of IL/CuO-rGNR/CPE (B)

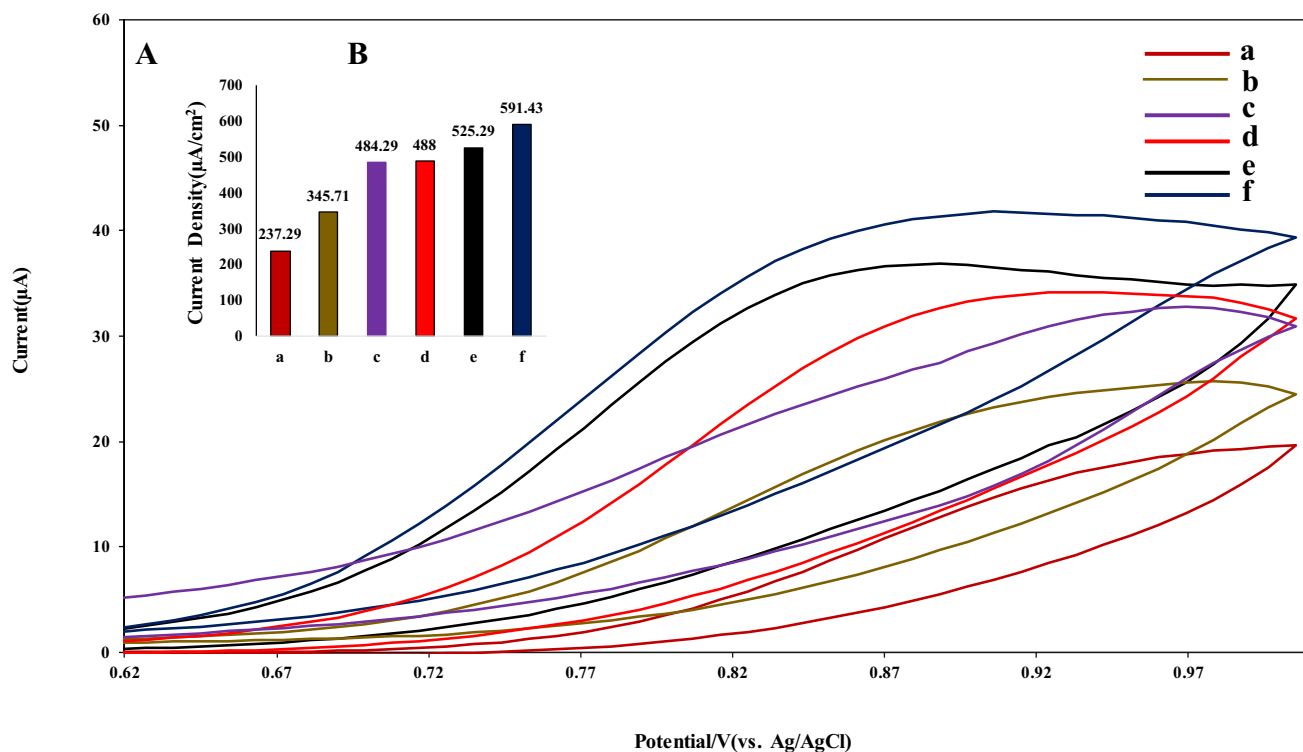


Fig. 3 A CV and the current density of CPE (a), CuO/CPE(b), GNR/CPE(c), CuO-GNR/CPE (d), IL/CPE(e), IL/CuO-rGNR/CPE (f) in the presence of 500 μM Tramadol at pH 7.0, scan rate 50 mV s^{-1} , respectively. (insert image: current density (B))

which was related to higher electrical conductivity and greater sensitivity for electrochemical investigations. Graphene nanomaterials like GNR and metal nanocomposites

can have inherent advantages of high ratio of surface area to weight, high exposure surface atoms, and fast charge transport properties. The space and channels between the layers

can significantly boost ions or/and reactants availability and makes significantly diffusion of electrode. To investigate the electrocatalytic mechanism of Tramadol at surface of IL/CuO-rGNR/CPE, CV was used at different scan rates of 20, 30, 50, 70, 90, 100 and 120 mVs^{-1} . Figure 4 demonstrated a linear relation between I_{pa} and square roots of scan rates from 20 to 120 mVs^{-1} which indicated the electrocatalytic relation behavior of Tramadol at surface of IL/CuO-rGNR/CPE was under diffusion process. As can be seen, there was a negative peak potential shift with an increase in the scan rate, which confirmed the irreversibility of the electrochemical reaction. Also, with the slope equal to $2.3RT/n(1-\alpha)F$ regarded to the Tafel plot, the electron transfer coefficient (α) was obtained about 0.8 ($\alpha=0.8$), which confirmed the presence of an irreversible electro-oxidation reaction.

Figure 5, shows the chronoamperometric tests of 100, 200, 300 and 400 μM Tramadol (pH 7.0) at the surface of sensor proposed (IL/CuO-rGNR/CPE). At experimental condition, the electron transfer rate of Tramadol was higher than diffusion rate to the surface of IL/CuO-rGNR/CPE. Under this condition, the electrochemical reaction of Tramadol as an electroactive species was obtained through Cottrell equation ($I = nFAD^{1/2}C\pi^{-1/2}t^{-1/2}$). Besides, a linear relationship in plot I vs. $t^{-1/2}$ indicated that by the related slopes that were attained from these curves, and according Cottrell equation

with $F = 96,485 \text{ C mol}^{-1}$, $n = 2$ and $A = 0.7 \text{ cm}^2$ the diffusion coefficient was calculated as $1.14 \times 10^{-7} \text{ cm}^2\text{s}^{-1}$.

EIS technique was used to examine the surface behavior of CPE electrode and different modified electrodes in presence of 5 mM of probe solution ($[\text{Fe}(\text{CN})_6]^{3-/4-}$) and KCl (0.1 M). Electron transfer resistance (R_{ct}) determined by diameter of the semicircle of the Nyquist diagram. According to Fig. 6, the largest diameter of the semicircle was assigned to CPE with largest R_{ct} and the lowest electron transfer resistance was referred to the IL/CuO-rGNR/CPE. R_{ct} values of CPE, CuO/CPE, GNR/CPE, CuO-rGNR/CPE, IL/CPE and IL/CuO-rGNR/CPE was calculated as 317, 143, 111, 86, 74 and 36, respectively. This was due to the synergistic effect of IL and CuO-rGNR, which improved the electrical conductivity and, therefore, reduced the charge transfer resistance at the modified electrode. So IL/CuO-rGNR/CPE was chosen for using in electrochemical measurements.

3.3 Linear range and detection limit investigation

DPV technique was applied to study the sensitivity of suggested sensor for measuring of Tramadol (Fig. 7). According to the recorded oxidation peak versus concentration of Tramadol (0.08, 1, 5, 10, 15, 30, 50, 70, 90, 100, 300, 500, 700 and 900 μM) as the concentration increased, the related I_{p}

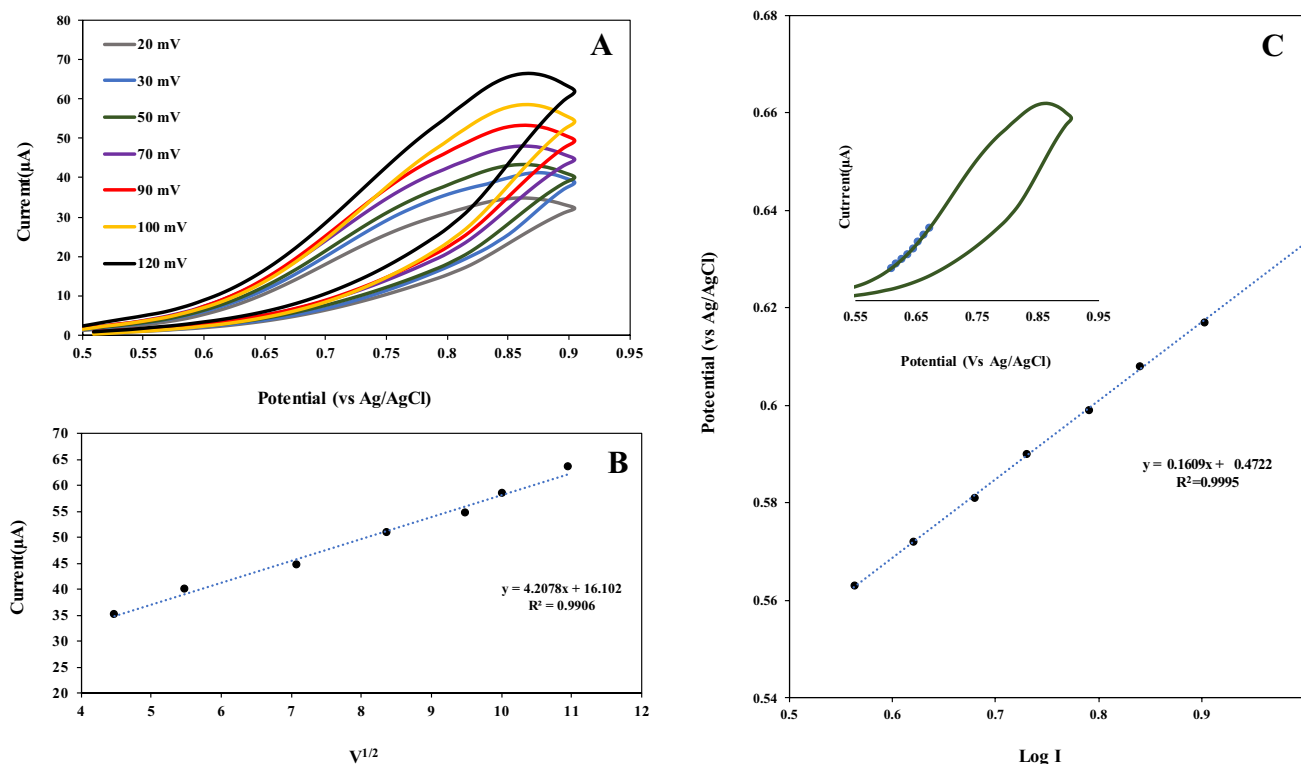


Fig. 4 **A** CV of Tramadol at IL/CuO-rGNR/CPE at different scan rates (from inner to outer) of 20, 30, 50, 70, 90, 100 and 120 mVs^{-1} , respectively, in PBS (0.1 M, pH 7.0). **B** Plot of I_{pa} versus ν for the

oxidation current of Tramadol at IL/CuO-rGNR/CPE. The voltammogram. **C** Tafel plot for Tramadol at IL/CuO-rGNR/CPE with scan rate of 50.0 mVs^{-1} in the presence of 500 μM Tramadol

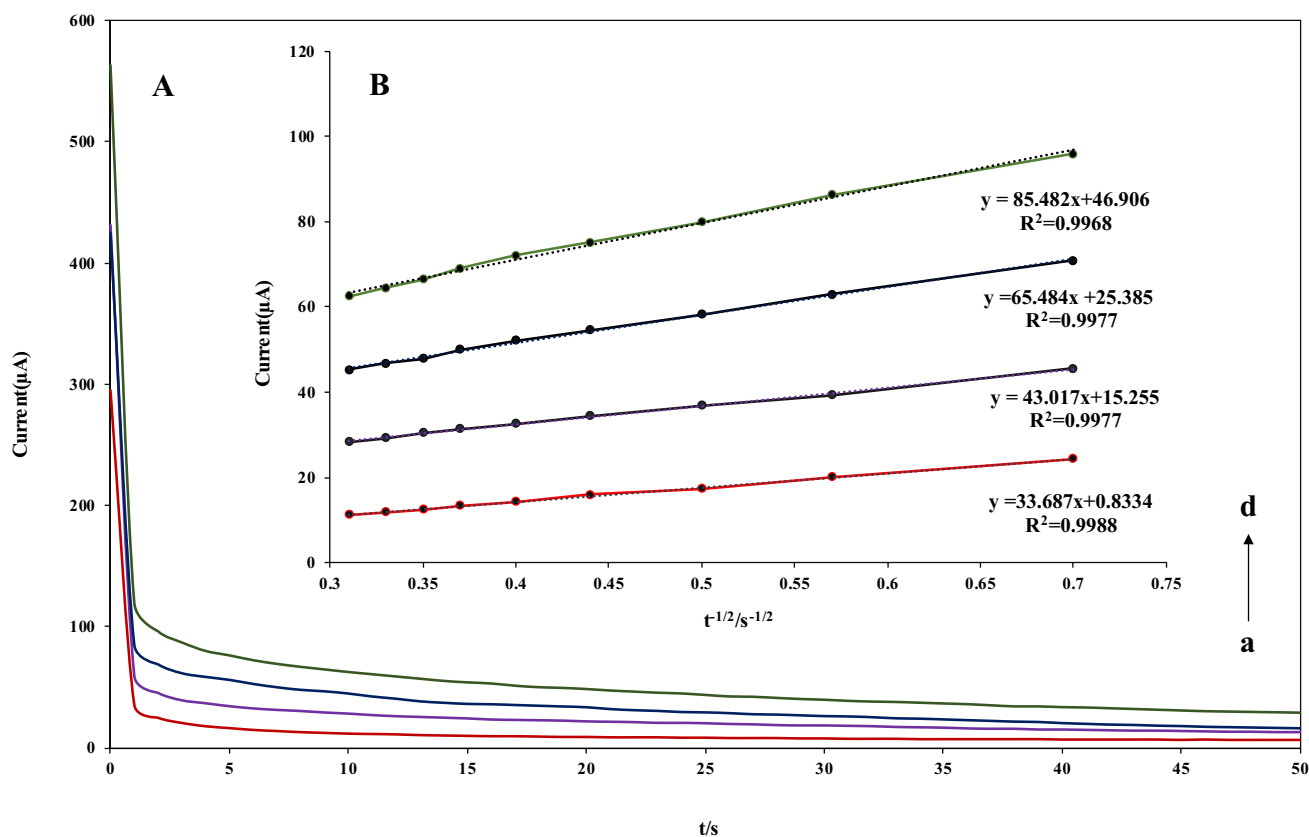


Fig. 5 **A** Chronoamperograms performed at IL/CuO-rGNR/CPE in the presence of 100.0, 200.0, 300.0 and 400.0 μM Tramadol in PBS (pH 7.0) (**a**→**d**). **B** Cottrell's plot

was raised over the two concentration range of 0.08–100 and 100–900 μM with various slopes. According to the equation ($\text{LOD} = 3\text{Sb}/m$), the LOD was attained as 0.05 μM . the comparison of the results of this investigation with other studies demonstrated in Table 1.

3.4 Simultaneous determination of tramadol, acetaminophen and olanzapine

The determination of Tramadol in the presence of Olanzapine and Acetaminophen by IL/CuO-rGNR/CPE was one of the main purpose of this study. According to Fig. 8, to evaluate the simultaneous determination, three separate cathode peak currents at 0.2 and 0.44 and 0.9 V potentials was obtained which referred to the oxidation of Olanzapine, Acetaminophen and Tramadol, by DPV curves at various concentrations of these drugs, respectively. It can be concluded the measuring of Tramadol in presence of Olanzapine and Acetaminophen was possible without significant interference.

3.5 Selectivity investigations

To investigate the selectivity of the technique used, different foreign species which can be affected on the Tramadol signal was investigated by DPV technique. The results are demonstrated in Table. 2. The result was indicated that no apparent interference was observed in the Tramadol analysis by adding foreign substrates. The stability of suggested sensor was evaluated by DPV of 500 μM of Tramadol after 2 weeks. The obtained responses were demonstrated the change of I_p were about 4.7%, which indicated acceptable stability of the suggested sensor.

3.6 Real sample analysis

The capability of IL/CuO-rGNR/CPE as a sensor for electrochemical investigations in real sample was performed by DPV and standard addition methods. Because the tissue of biological sample was complex, the standard addition technique was used to determine. For this purpose, real samples containing various concentration of Tramadol was

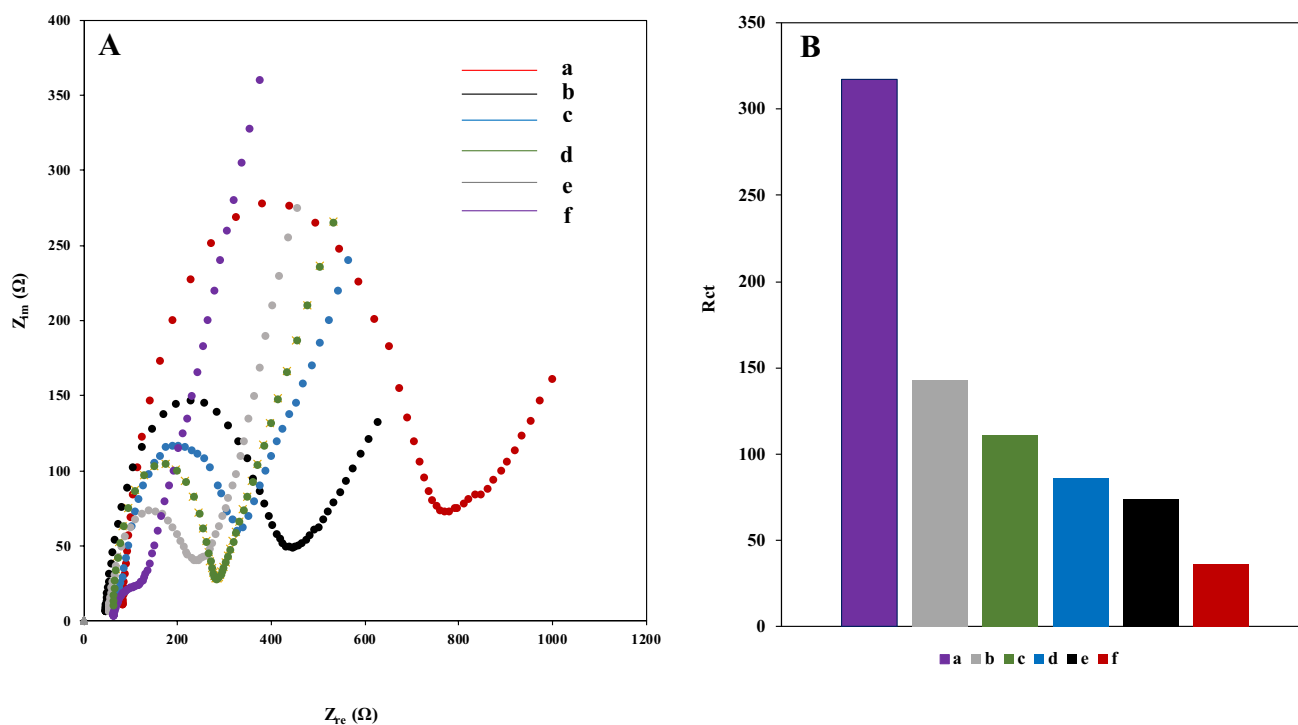


Fig. 6 A Nyquist diagrams of CPE (a), CuO /CPE (b), GNR/CPE (c), CuO-GNR/CPE (d), IL/CPE (e), IL/CuO-rGNR/CPE (f) electrodes (from inner to outer) in 5.0 mmol L⁻¹ [Fe(CN)₆]^{3-/4-} in 0.1 mol L⁻¹ KCl. B The related R_{ct} values

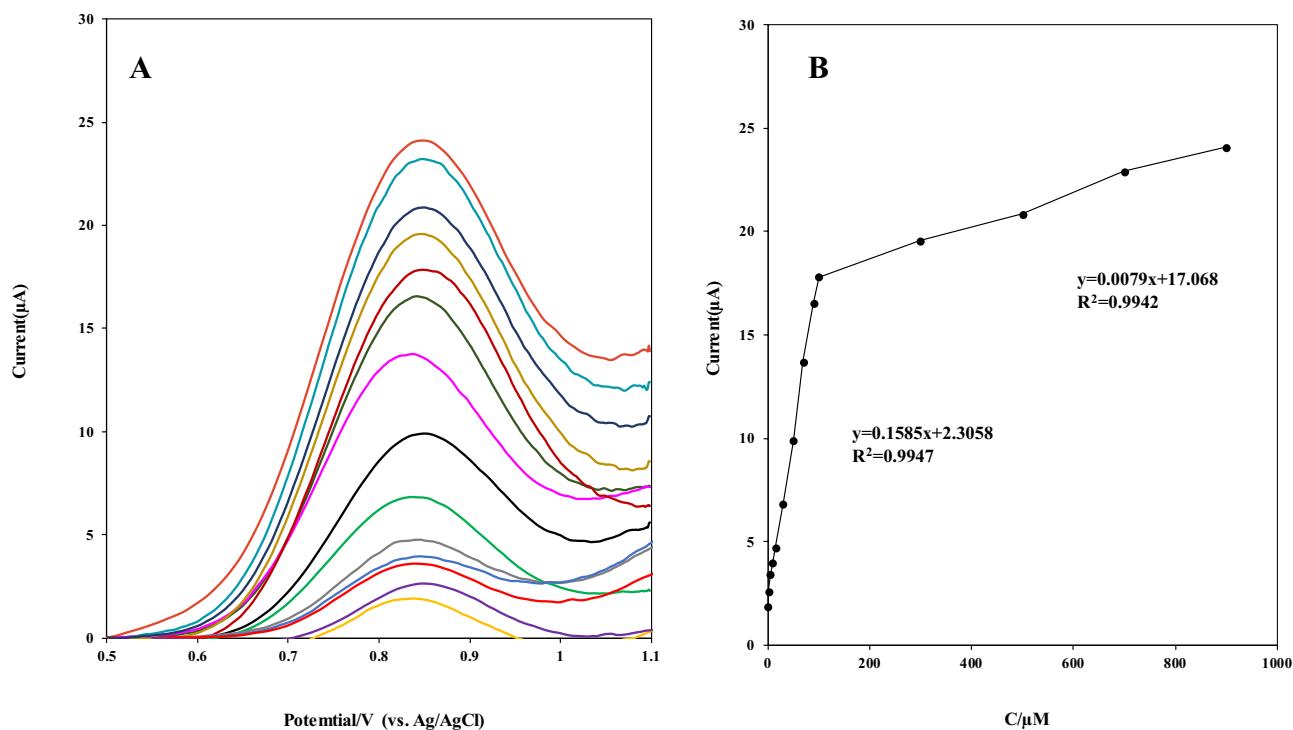


Fig. 7 A DPVs for various concentrations of Tramadol (0.08, 1, 5, 10, 15, 30, 50, 70, 90, 100, 300, 500, 700 and 900 μM) in the range of range 0.08 to 900.0 μM at surface of IL/CuO-rGNR/CPE at pH

7.0 and scan rate: 50 mV s⁻¹. B Plots of linear range as a function of Tramadol concentration

Table 1 Comparison of this study with other works

Nano composite	Electrode	Limit of detection (μM)	Linear range (μM)	Reference
La ³⁺ /ZnO NF-MWCNT	CPE	0.08	0.5–800	1
CoO@f-CNT	GCE	0.449	1–300	2
SnO ₂ / α -Fe ₂ O ₃	CPE	0.006	0.5–65	3
HTP-Au NPs/GN	CPE	0.82	1–100	4
1-M-3-BBR/PR(OH)3-GQD	CPE	0.003	0.009–100	5
H-GONPs	GCE	0.015	0.08–200	6
Sb ₂ O ₃ NPs/MWCNT	GCE	0.095	0.04 -18	7
IL/CuO-rGNR	CPE	0.05	0.08–900	This work

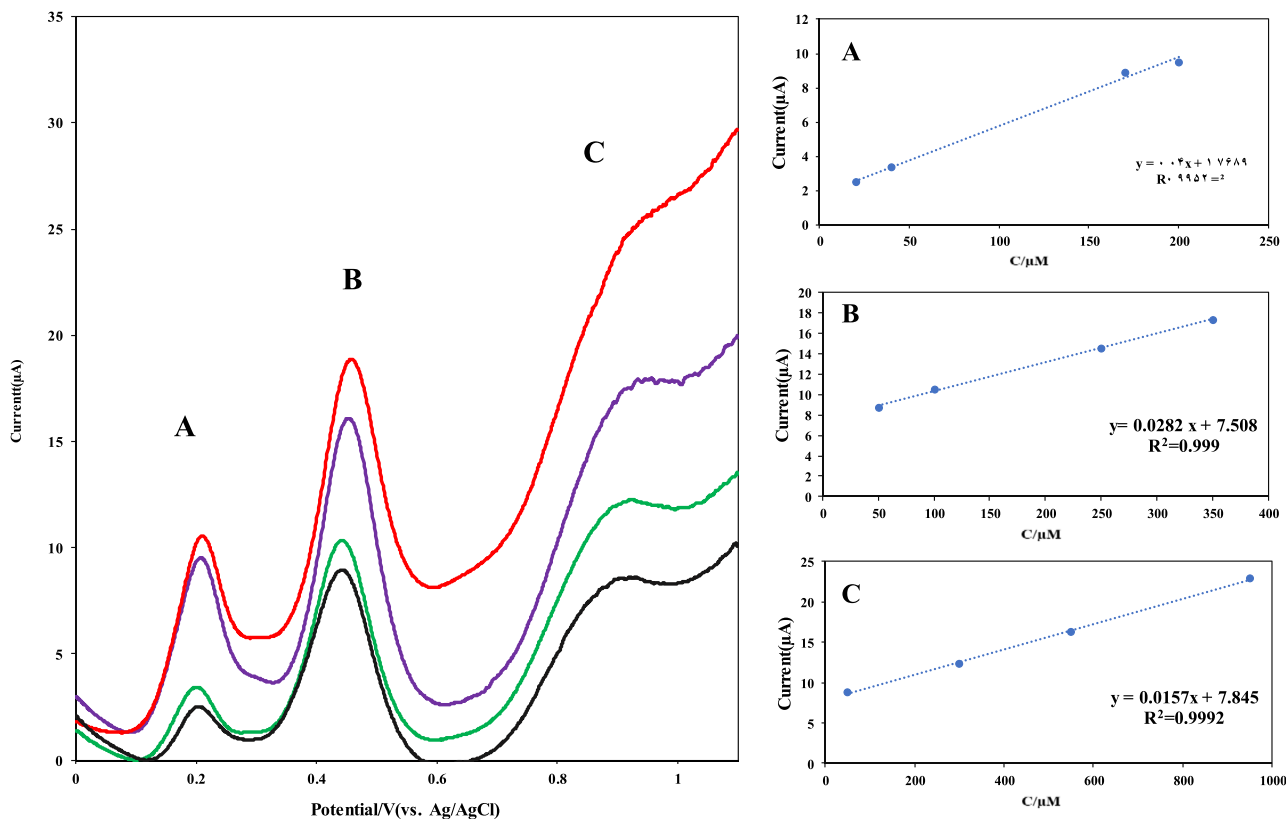


Fig. 8 The DPVs of IL/CuO-rGNR/CPE at different concentrations of (A) Olanzapine, (B) Acetaminophen and (C) Tramadol solutions with (A): 20.0+40.0+170.0+200.0; (B): 100.0+150.0+300.0+400.0; (C): 50.0+300.0+550.0+950.0 μM , respectively, at pH 7.0 phosphate buffer

Table 2 Interference investigates data for analysis of 500 μM Tramadol

Species	Tolerant limits ($W_{\text{substances}}/W_{\text{Analytes}}$)
Na ⁺ , K ⁺ , Ca ²⁺ , NH ₄ ⁺ , Mg ²⁺ , Cl ⁻ , I ⁻ , SO ₄ ²⁻	500
NO ₃ ⁻ , PO ₄ ³⁻ , F ⁻ , CO ₃ ²⁻	500
Glucose, sucrose, urea, uric acid	400
Ascorbic acid	300
Glycine, valine and Starch	600

Table 3 Investigation of Tramadol in real samples

Sample	Standard solution added(μM)	Determined (μM)	Recovery (%)	RSD
(a) Human plasma				
1	0	6.175 ± 0.275	–	–
2	20	26.425 ± 0.71	101.25	2.53
3	40	45.98 ± 0.329	99.51	0.65
4	60	66.55 ± 0.57	100.62	0.81
5	80	85.65 ± 0.617	99.34	0.99
(b) Human urine				
1	0	4.125 ± 0.262	–	–
2	20	24.79 ± 0.469	103.32	1.77
3	40	44.88 ± 0.341	101.88	0.71
4	60	64.4 ± 0.88	100.45	1.27
5	80	83.93 ± 0.55	99.75	0.62
(c) Tablet				
1	0	5.05 ± 0.23	–	–
2	20	25.24 ± 0.533	100.95	1.98
3	40	45.66 ± 0.652	101.52	1.34
4	60	65.6 ± 0.876	100.91	1.25
5	80	84.87 ± 0.724	99.77	0.8

examined using proposed sensor. Real sample preparation was done as mentioned in Sect. 2.5. The observed results are listed in Table. 3 which confirmed the IL/CuO-rGNR/CPE can be used to determine the Tramadol in biological samples.

3.7 Reproducibility and stability

The stability of IL/CuO-rGNR/CPE was evaluated by repeating eight consecutive measurements for 500 μM Tramadol in PBS at scan rate 50 mV s^{-1} . No observable change in peak current was obtained, that affirmed that IL/CuO-rGNR/CPE was greatly stable. The relative standard deviations (RSD) was obtained to be below 5% representing a suitable reproducibility. Also after CPE modifying which was kept for 10 days, an improvement by 5% in the oxidation peak of 500 μM Tramadol was attained. These results can be related to the high stability of IL/CuO-rGNR/CPE sensor compared to other evaluates with other modified electrodes.

4 Conclusions

In this work, simultaneous determination of Tramadol, Acetaminophen and Olanzapine using IL/CuO-rGNR/CPE nanocomposite as a sensitive sensor was suggested for the first time. According to the responses, the synergistic influence of CuO-rGNR and IL increased the electrical conductivity, catalytic activity and surface area accessible for these drugs at the suggested electrode that can considerably improve electron transfer. Under optimum conditions, the IL/CuO-rGNR/CPE electrode displayed wide linear range, about 0.05 μM and 0.08–900.0 μM and low detection limit (LOD) was achieved to be 0.05 μM , respectively. Furthermore, the value of $\alpha = 0.8$ and $D = 1.14 \times 10^{-7} \text{ cm}^2 \text{ s}^{-1}$ was achieved for Tramadol. The obtained results to evaluate the sensitivity demonstrated the change of I_p were about 4.7%, which designated acceptable stability of the proposed sensor. The responses have illustrated the ability of suggested sensor in real samples with satisfied results.

Author contribution HS: Investigation, MS-N: Supervision, Validation, AR-V: Supervision, Investigation, RD: Investigation, Roles/Writing – original draft.

Data availability The datasets generated and analyzed during the current study are available from the corresponding author on reasonable request.

Declarations

Conflict of interest The authors declare that they have no known competing financial interests or personal relationships that could have appeared to influence the work reported in this paper.

References

- Ricardo-Teixeira Tarley C, de Cássia Mendonça J, Rianne da Rocha L, Boareto Capelari T, Carolyne Prete M, Cecílio Fonseca M, Midori de-Oliveira F, César Pereira A, Luiz Scheel G, Bastos Borges K, Gava Segatelli M (2020) Development of a molecularly imprinted poly(acrylic acid)-MWCNT nanocomposite electrochemical sensor for tramadol determination in pharmaceutical samples. *Electroanalysis* 32:1130–1137. <https://doi.org/10.1002/elan.201900148>
- Pereira FJ, Rodríguez-Cordero A, López R, Robles LC, Aller AJ (2021) Development and validation of an rp-hplc-pda method for determination of paracetamol, caffeine and tramadol hydrochloride in pharmaceutical formulations. *Pharmaceuticals*. <https://doi.org/10.3390/ph14050466>
- Patteet L, Morrens M, Maudens KE, Niemegeers P, Sabbe B, Neels H (2012) Therapeutic drug monitoring of common antipsychotics. *Ther Drug Monit* 34:629–651. <https://doi.org/10.1097/FTD.0b013e3182708ec5>
- Mohammadi-Behzad L, Gholivand MB, Shamsipur M, Gholivand K, Barati A, Gholami A (2016) Highly sensitive voltammetric sensor based on immobilization of

- bisphosphoramidate-derivative and quantum dots onto multi-walled carbon nanotubes modified gold electrode for the electrocatalytic determination of olanzapine. *Mater Sci Eng C* 60:67–77. <https://doi.org/10.1016/j.msec.2015.10.068>
5. Rouhani M, Soleymanpour A (2019) A new selective carbon paste electrode for potentiometric analysis of olanzapine. *Meas J Int Meas Confed* 140:472–478. <https://doi.org/10.1016/j.measurement.2019.04.018>
 6. Muthusankar A, Sangili SM, Chen R, Karkuzhali M, Sethupathi G, Gopu S, Karthick RK, Devi N (2018) Sengottuvelan, In situ assembly of sulfur-doped carbon quantum dots surrounded iron(III) oxide nanocomposite; a novel electrocatalystanesan for highly sensitive detection of antipsychotic drug olanzapine. *J Mol Liq* 268:471–480. <https://doi.org/10.1016/j.molliq.2018.07.059>
 7. Filik H, Avan AA, Aydar S, Çetintaş G (2014) Determination of acetaminophen in the presence of ascorbic acid using a glassy carbon electrode modified with poly(Caffeic acid). *Int J Electrochem Sci* 9:148–160
 8. Jahani PM, Mohammadi SZ, Khodabakhshzadeh A, Asl MS, Jang HW, Shokouhimehr M, Zhang K, Van Le Q, Peng W (2020) Simultaneous voltammetric detection of acetaminophen and tramadol using molybdenum tungsten disulfide-modified graphite screen-printed electrode. *Int J Electrochem Sci* 15:9024–9036. <https://doi.org/10.20964/2020.09.12>
 9. Shi H, Zheng Y, Karimi-Maleh H, Fu L (2021) Alginate-modified Cassava fiber loaded palladium for electrochemical paracetamol analysis. *Int J Electrochem Sci* 16:1–10. <https://doi.org/10.20964/2021.10.24>
 10. Islam MM, Arifuzzaman M, Rushd S, Islam MK, Rahman MM (2022) Electrochemical sensor based on poly (aspartic acid) modified carbon paste electrode for paracetamol determination. *Int J Electrochem Sci*. <https://doi.org/10.20964/2022.02.39>
 11. Zheng B, He X, Zhang Q, Duan M (2022) A novel molecularly imprinted membrane for highly sensitive electrochemical detection of paracetamol. *Int J Electrochem Sci* 17:1–11. <https://doi.org/10.20964/2022.07.37>
 12. Beakley BD, Kaye AM, Kaye AD (2015) Tramadol, pharmacology, side effects, and serotonin syndrome: a review. *Pain Physician* 18:395–400. <https://doi.org/10.36076/ppj.2015/18/395>
 13. Dahshan HE, Helal MA, Mostafa SM, Elgawish MS (2019) Development and validation of an HPLC-UV method for simultaneous determination of sildenafil and tramadol in biological fluids: Application to drug-drug interaction study. *J Pharm Biomed Anal* 168:201–208. <https://doi.org/10.1016/j.jpba.2019.02.025>
 14. Atila Karaca S, Yeniceli Uğur D (2018) Development of a validated hplc method for simultaneous determination of olanzapine and aripiprazole in human plasma, Marmara. *Pharm J* 22:493–501. <https://doi.org/10.12991/jrp.2018.90>
 15. Tanaka H, Naito T, Mino Y, Kawakami J (2016) Validated determination method of tramadol and its desmethylates in human plasma using an isocratic LC-MS/MS and its clinical application to patients with cancer pain or non-cancer pain. *J Pharm Heal Care Sci* 2:1–9. <https://doi.org/10.1186/s40780-016-0059-2>
 16. Lu W, Zhao S, Gong M, Sun L, Ding L (2018) Simultaneous determination of acetaminophen and oxycodone in human plasma by LC-MS/MS and its application to a pharmacokinetic study. *J Pharm Anal* 8:160–167. <https://doi.org/10.1016/j.jpba.2018.01.006>
 17. Khelifi A, Azzouz M, Abtroun R, Reggabi M, Alamir B (2018) Sulpiride in human plasma by liquid chromatography/tandem mass spectrometry (LC-MS/MS). *Res Artic Determ Chlorpromazine* 2018:1–13. <https://doi.org/10.1155/2018/5807218>
 18. Kimani MM, Lanzarotta A, Batson JCS (2021) Trace level detection of select opioids (fentanyl, hydrocodone, oxycodone, and tramadol) in suspect pharmaceutical tablets using surface-enhanced Raman scattering (SERS) with handheld devices. *J Forensic Sci* 66:491–504. <https://doi.org/10.1111/1556-4029.14600>
 19. Alharbi O, Xu Y, Goodacre R (2015) Detection and quantification of the opioid tramadol in urine using surface enhanced Raman scattering. *Analyst* 140:5965–5970. <https://doi.org/10.1039/c5an01177a>
 20. Al-Otaibi JS, Albrycht P, Mary YS, Mary YS, Książkowska-Gocalska M (2021) Concentration-dependent SERS profile of olanzapine on silver and silver-gold metallic substrates. *Chem Pap* 75:6059–6072. <https://doi.org/10.1007/s11696-021-01783-9>
 21. Sefaty B, Masrounia M, Eshaghi Z, Bozorgmehr MR (2021) Determination of tramadol and fluoxetine in biological and water samples by magnetic dispersive solid-phase microextraction (MDSPME) with gas chromatography-mass spectrometry (GC-MS). *Anal Lett* 54:884–902. <https://doi.org/10.1080/00032719.2020.1786695>
 22. Adegoke OA, Thomas OE, Emmanuel SN (2016) Colorimetric determination of olanzapine via charge-transfer complexation with chloranilic acid. *J Taibah Univ Sci* 10:651–663. <https://doi.org/10.1016/j.jtusc.2015.12.002>
 23. Shihana F, Dissanayake D, Dargan P, Dawson A (2010) A modified low-cost colorimetric method for paracetamol (acetaminophen) measurement in plasma. *Clin Toxicol* 48:42–46. <https://doi.org/10.3109/15563650903443137>
 24. Khairy M, Banks CE (2020) A screen-printed electrochemical sensing platform surface modified with nanostructured ytterbium oxide nanoplates facilitating the electroanalytical sensing of the analgesic drugs acetaminophen and tramadol. *Microchim Acta*. <https://doi.org/10.1007/s00604-020-4118-x>
 25. Ghorbani-Bidkorbeh F, Shahrokhian S, Mohammadi A, Dinarvand R (2010) Simultaneous voltammetric determination of tramadol and acetaminophen using carbon nanoparticles modified glassy carbon electrode. *Electrochim Acta* 55:2752–2759. <https://doi.org/10.1016/j.electacta.2009.12.052>
 26. Arabali V, Malekmohammadi S, Karimi F (2020) Surface amplification of pencil graphite electrode using CuO nanoparticle/polypyrrole nanocomposite; a powerful electrochemical strategy for determination of tramadol. *Microchem J* 158:105179. <https://doi.org/10.1016/j.microc.2020.105179>
 27. Kolahi-Ahari S, Deiminiat B, Rounaghi GH (2020) Modification of a pencil graphite electrode with multiwalled carbon nanotubes capped gold nanoparticles for electrochemical determination of tramadol. *J Electroanal Chem* 862:113996. <https://doi.org/10.1016/j.jelechem.2020.113996>
 28. Rao L, Zhu Y, Duan Z, Xue T, Duan X, Wen Y, Kumar AS, Zhang W, Xu J, Hojjati-Najafabadi A (2022) Lotus seedpods biochar decorated molybdenum disulfide for portable, flexible, outdoor and inexpensive sensing of hyperin. *Chemosphere* 301:134595. <https://doi.org/10.1016/j.chemosphere.2022.134595>
 29. Monsef R, Salavati-Niasari M (2021) Hydrothermal architecture of Cu₅V₂O₁₀ nanostructures as new electro-sensing catalysts for voltammetric quantification of mefenamic acid in pharmaceuticals and biological samples. *Biosens Bioelectron* 178:113017. <https://doi.org/10.1016/j.bios.2021.113017>
 30. Mansoorianfar M, Nabipour H, Pahlevani F, Zhao Y, Hussain Z, Hojjati-Najafabadi A, Hoang HY, Pei R (2022) Recent progress on adsorption of cadmium ions from water systems using metal-organic frameworks (MOFs) as an efficient class of porous materials. *Environ Res* 214:114113. <https://doi.org/10.1016/j.envres.2022.114113>
 31. Baladi E, Davar F, Hojjati-Najafabadi A (2022) Synthesis and characterization of g-C₃N₄-CoFe₂O₄-ZnO magnetic nanocomposites for enhancing photocatalytic activity with visible light for

- degradation of penicillin G antibiotic. *Environ Res* 215:114270. <https://doi.org/10.1016/j.envres.2022.114270>
32. Hojjati-Najafabadi A, Rahmanpour MS, Karimi F, Zabihi-Feyzaba H, Malekmohammad S, Agarwal S, Gupta VK, Khalilzadeh MA (2020) Determination of tert-butylhydroquinone using a nanostructured sensor based on CdO/SWCNTs and ionic liquid. *Int J Electrochem Sci* 15:6969–6980. <https://doi.org/10.20964/2020.07.85>
 33. Hojjati-Najafabadi A, Aygun A, Tiri RNE, Gulbagca F, Lounissaa MI, Feng P, Karimi F, Sen F (2022) *Bacillus thuringiensis* based ruthenium/nickel Co-doped zinc as a green nanocatalyst: enhanced photocatalytic activity, mechanism, and efficient H₂ production from sodium borohydride methanolysis. *Ind Eng Chem Res*. <https://doi.org/10.1021/acs.iecr.2c03833>
 34. Bijad M, Hojjati-Najafabadi A, Asari-Bami H, Habibzadeh S, Amini I, Fazeli F (2021) An overview of modified sensors with focus on electrochemical sensing of sulfite in food samples. *Eurasian Chem Commun* 3:116–138. <https://doi.org/10.22034/ecc.2021.268819.1122>
 35. Hojjati-Najafabadi A, Salmanpour S, Sen F, Asrami PN, Mahdavian M, Khalilzadeh MA (2022) A tramadol drug electrochemical sensor amplified by biosynthesized au nanoparticle using mentha aquatic extract and ionic liquid. *Top Catal* 65:587–594. <https://doi.org/10.1007/s11244-021-01498-x>
 36. Chen D, Feng H, Li J, Al-Nafiey AKH, Lin F, Tong X, Wang Y, Bao J, Wang ZM, Marcano DC, Kosynkin DV, Berlin JM, Sinitkii A, Sun Z, Slesarev AS, Alemany LB, Lu W, Tour JM (2015) Reduced graphene oxide-based nanocomposites: synthesis, characterization and applications. *Nanoscale Res Lett* 12:2078–2078. <https://doi.org/10.1021/acs.nano.8b00128>
 37. Karimi-Maleh H, Darabi R, Karimi F, Karaman C, Shahidi SA, Zare N, Baghayeri M, Fu L, Rostamnia S, Rouhi J, Rajendran S (2023) State-of-art advances on removal, degradation and electrochemical monitoring of 4-aminophenol pollutants in real samples: a review. *Environ Res* 222:115338. <https://doi.org/10.1016/j.envres.2023.115338>
 38. Hojjati-Najafabadi A, Mansoorianfar M, Liang T, Shahin K, Karimi-Maleh H (2022) A review on magnetic sensors for monitoring of hazardous pollutants in water resources. *Sci Total Environ* 824:153844. <https://doi.org/10.1016/j.scitotenv.2022.153844>
 39. Buledi JA, Mahar N, Mallah A, Solangi AR, Palabiyik IM, Qambrani N, Karimi F, Vasseghian Y, Karimi-Maleh H (2022) Electrochemical quantification of mancozeb through tungsten oxide/reduced graphene oxide nanocomposite: a potential method for environmental remediation. *Food Chem Toxicol* 161:112843. <https://doi.org/10.1016/j.fct.2022.112843>
 40. Cheraghi S, Taher MA, Karimi-Maleh H, Karimi F, Shabani-Nooshabadi M, Alizadeh M, Al-Othman A, Erk N, Yegya Raman PK, Karaman C (2022) Novel enzymatic graphene oxide based biosensor for the detection of glutathione in biological body fluids. *Chemosphere* 287:132187. <https://doi.org/10.1016/j.chemosphere.2021.132187>
 41. Avinash B, Ravikumar CR, Kumar MRA, Nagaswarupa HP, Santosh MS, Bhatt AS, Kuznetsov D (2019) Nano CuO: electrochemical sensor for the determination of paracetamol and D-glucose. *J Phys Chem Solids* 134:193–200. <https://doi.org/10.1016/j.jpcs.2019.06.012>
 42. Li Y, Cheng C, Yang YP, Dun XJ, Gao J, Jin XJ (2019) A novel electrochemical sensor based on CuO/H-C₃N₄/rGO nanocomposite for efficient electrochemical sensing nitrite. *J Alloys Compd* 798:764–772. <https://doi.org/10.1016/j.jallcom.2019.05.137>
 43. Terrones M, Botello-Méndez AR, Campos-Delgado J, López-Urías F, Vega-Cantú YI, Rodríguez-Macías FJ, Elías AL, Muñoz-Sandoval E, Cano-Márquez AG, Charlier JC, Terrones H (2010) Graphene and graphite nanoribbons: morphology, properties, synthesis, defects and applications. *Nano Today* 5:351–372. <https://doi.org/10.1016/j.nantod.2010.06.010>
 44. Liu J, Liu Z, Barrow CJ, Yang W (2015) Molecularly engineered graphene surfaces for sensing applications: a review. *Anal Chim Acta* 859:1–19. <https://doi.org/10.1016/j.aca.2014.07.031>
 45. Swamy NK, Mohana KNS, Hegde MB, Madhusudana AM, Rajitha K, Nayak SR (2021) Fabrication of graphene nanoribbon-based enzyme-free electrochemical sensor for the sensitive and selective analysis of rutin in tablets. *J Appl Electrochem* 51:1047–1057. <https://doi.org/10.1007/s10800-021-01557-x>
 46. Darabi R, Shabani-Nooshabadi M, Khoobi A (2021) A potential strategy for simultaneous determination of deferoxamine and vitamin C using MCR-ALS with nanostructured electrochemical sensor in serum and urine of Thalassemia and diabetic patients. *J Electrochem Soc* 168:46514. <https://doi.org/10.1149/1945-7111/abf6ed>
 47. Karimi-Maleh H, Sheikhsheoie M, Sheikhsheoie I, Ranjbar M, Alizadeh J, Maxakato NW, Abbaspourrad A (2019) A novel electrochemical epinine sensor using amplified CuO nanoparticles and a: N-hexyl-3-methylimidazolium hexafluorophosphate electrode. *New J Chem* 43:2362–2367. <https://doi.org/10.1039/c8nj05581e>
 48. Matsumoto H, Imaizumi S, Konosu Y, Ashizawa M, Minagawa M, Tanioka A, Lu W, Tour JM (2013) Electrospun composite nanofiber yarns containing oriented graphene nanoribbons. *ACS Appl Mater Interfaces* 5:6225–6231. <https://doi.org/10.1021/am401161b>
 49. Shang S, Gan L, Yuen CWM, Jiang SX, Luo NM (2015) The synthesis of graphene nanoribbon and its reinforcing effect on poly (vinyl alcohol). *Compos Part A* 68:149–154. <https://doi.org/10.1016/j.compositesa.2014.10.011>
 50. Abdel-Aal SK, Beskrovnyi AI, Ionov AM, Mozchil RN, Abdel-Rahman AS (2021) Structure investigation by neutron diffraction and X-ray diffraction of graphene nanocomposite CuO-rGO prepared by low-cost method. *Phys Status Solidi Appl Mater Sci* 218:1–9. <https://doi.org/10.1002/pssa.202100138>

Publisher's Note Springer Nature remains neutral with regard to jurisdictional claims in published maps and institutional affiliations.

Springer Nature or its licensor (e.g. a society or other partner) holds exclusive rights to this article under a publishing agreement with the author(s) or other rightsholder(s); author self-archiving of the accepted manuscript version of this article is solely governed by the terms of such publishing agreement and applicable law.